Weld Penetration Sensitivity to Welding Variables When Near Full Joint Penetration

Slight variations in welding parameters can cause wide fluctuations in results under near full joint penetration conditions

BY P. BURGARDT AND C. R. HEIPLE

ABSTRACT. The sensitivity of penetration to current, travel speed, and thickness are reported for GTA welds near full joint penetration in 304L stainless steel. Near full penetration, weld depth is much more sensitive to welding conditions than far from full penetration. For example, penetration increased four times faster with increasing current near full penetration than far from full penetration. Similar results were obtained for keyhole mode electron beam welds near full penetration as a function of beam power. Experimental results are in reasonable agreement with predictions from exact solutions to the conduction equations for finite thickness plate using a point heat source. Excellent agreement is achieved when the arc is treated as a distributed rather than a point heat source. Experimental agreement with line source predictions is also excellent for electron beam welds because a tightly focused electron beam is closely approximated by a line heat source.

Introduction

Design of weldments normally calls for full penetration welds with verifiable drop-through or for welds with joint penetration significantly less than the part thickness. The sensitivity of joint penetration to welding variables is reasonably well understood in both cases. Recently, we have observed several examples of unusual weld instability when the design weld penetration is nearly identical to the part thickness. One example is a multipass weld in which complete remelting (full root penetration) of the root pass during the second pass is not allowed. Another example is the situation where full penetration is required, but only minimal drop-through is allowed. In these situations, the sensitivity of weld penetration to changes in process variables is great. Presumably these are somewhat unusual situations as there has been little mention of these problems in the literature. However, with the introduction of high-precision welding equipment, it has become feasible to require welds of this nature and the ramifications of this must be clearly understood.

The unusually high sensitivity of penetration to process variables for near full joint penetration welds is a result of heat flow modifications by the part back surface. As the weld nears full penetration, the back surface acts like an insulating barrier and heat flow changes from three-dimensional (3-D) toward less efficient two-dimensional (2-D) character. Reduced heat transfer means that more melting occurs at the root of the weld than would otherwise occur. This effect becomes increasingly important as full penetration is approached. Thus, large changes in joint penetration occur for subtle changes in the process variables.

KEY WORDS

Joint Penetration
Current
Travel Speed
GTAW
304L
Keyhole Mode EB
Electron Beam Weld
Beam Power
Heat Flow
Welding Conditions

P. BURGARDT and C. R. HEIPLE are with EG & G Rocky Flats Corp., Golden, Colo.

Heat Flow

The important weld characteristics of all fusion welds, such as fusion zone size and cooling rate, are determined by heat flow away from the welding heat source. Of course, heat flow phenomena are often very complex and defy simple analytical description. However, the essential aspects of heat flow in weldments are mostly well understood. Theoretical analyses of welds have concentrated on thick plates (3-D heat flow) or thin sheet (full joint penetration and 2-D heat flow). These two limiting cases are discussed in detail elsewhere (see for example Myers, *et al.*) (Ref. 1).

The simple analytical solution for 3-D heat flow describes the temperature field around a traveling point heat source in a semi-infinite plate; this is the Rosenthal equation (Ref. 2). Many practically important situations such as GTA and conduction-mode EB welds can be described by this solution. Christensen, *et al.* (Ref. 3), put the Rosenthal equation into a dimensionless form and showed that the overall size of the weldment is related to the operating parameter, n. This is a dimensionless grouping of terms from the Rosenthal equation and is given by:

$$n = \frac{Pv}{4\pi\kappa\alpha\left(T_f - T_o\right)} \qquad (1)$$

where P is the weld input power; v is the part travel speed; $\alpha = \kappa/\rho C$ is the thermal diffusivity of the material; κ is the thermal conductivity, ρC is the heat capacity; T_f Is the material melting point; and T_o is the ambient temperature.

Predictions of process variable sensitivities for purely 3-D heat flow behavior can be easily derived from the Rosenthal equation and these are in reasonable agreement with experimental weld

penetration data. For example, Savage, *et al.* (Ref. 4), measured partial penetration welds in mild steel and found the dependence of penetration on current, voltage, and travel speed to be in agreement with predictions from the Rosenthal equation. The material was thick enough so that penetration was essentially independent of part thickness.

Full joint penetration welds are described by 2-D heat flow, which is described as heat flow away from a traveling line source in a semi-infinite plate. A second equation from Rosenthal gives the line source solution (Ref. 2). The weld nugget dimensions are determined by an operating parameter that is given by:

$$n_2 = \frac{(P/t)}{2\pi\kappa(T_f - T_o)} \qquad (2)$$

In the intermediate regime, neither 2-D nor 3-D heat flow dominate and neither is an adequate description of the heat flow. For these welds, the sensitivity of weld penetration to the process parameters should change rapidly from one behavior to the other. That is, weld penetration should rapidly increase from that predicted by the Rosenthal equation to become equal to the plate thickness.

The point and line source analytical solutions for heat flow are only approximations because several simplifying assumptions were made in their derivation. Thus, predicted temperature distributions near the source are not realistic and actual weld pool shapes often differ substantially from those predicted. Furthermore, heat flow analyses typically do not give process variable sensitivities in a simple way near full penetration. The analytical solutions do give reasonable predictions of overall weld size and thermal history of the plate some distance from the weld pool. The analytic solution for 3-D heat flow can be improved by treating the source as distributed rather than as a point.

A limited theoretical analysis of the near full penetration problem has been done. For example, Myers, *et al.* (Ref. 1), discusses heat flow where the weld starts to feel the effects of the finite part thickness. They call this 2.5-D heat flow because it is intermediate between the normal 3-D and 2-D behaviors. They found that this effect starts to become important at about d > t/3, where d is weld penetration and t is part thickness. In an analysis of the related finite width problem, Roberts and Wells (Ref. 5) showed that part width is important if the part edge is within about 5w from the weld, where w is the weld top surface width. In a more recent paper, Malmuth, *et al.* (Ref. 6), presents calculations and experimental data for aluminum that show a buildup of heat on the back surface of thin plates. These results show an increase in weld penetration from about 50 to about 80% in 0.5-in. (12.7-mm) thick plates welded with and without a copper backing bar. A related experimental result is that of Friedman and Glickstein (Ref. 7). They showed that a stationary spot weld rapidly goes to full penetration when the baseline penetration exceeds about 0.2 t; sensitivities to welding variables are large in this range also. Finally, Alberry, *et al.* (Ref. 8), reported the distribution of penetrations achieved by many manual welders for thin section GMA tube attachment welds. The distribution of weld penetration achieved was close to a normal distribution, except that there was a significant deviation at the upper (high penetration) end of the distribution. This deviation almost certainly arises from the increase in penetration as full penetration is approached.

Much of the theoretical work on finite thickness effects has been associated with the related problem of the cooling rate in thin plates. For example, Jhaveri, *et al.* (Ref. 9), showed that the change from 3-D to 2-D heat flow behavior fundamentally changes part cooling rate. This behavior change is described by a characteristic part thickness,

$$t_o = \sqrt{P/\left[v\rho C\left(T_f - T_o\right)\right]} \qquad (3)$$

They found that 3-D analysis applies $T_o > 1$ and that 2-D analysis applies $T_o < 0.6$. In the intermediate regime there is a complex crossover behavior. A similar analysis accompanied with experimental cooling rate data was presented by Barry, *et al.* (Ref. 10). He showed that plate bottom surface temperature increases rapidly for w/t > 1.2. For a symmetric weld, this corresponds to weld penetration increasing anomalously for d/t = 0.6.

All of these papers clearly illustrate that weld penetration behavior changes considerably when a dimension of the welded part becomes comparable to the weld nugget dimensions. They also show that a large sensitivity of weld penetration to process parameters is possible for finite thickness parts. However, none of these papers explicitly considered process parameter effects.

For this paper, calculations of the effects of finite plate thickness on the heat

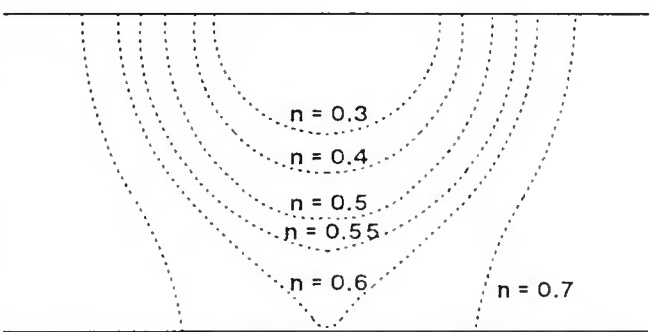

Fig. 1 — Calculated weld penetration for a 3-D heat flow weld (point source) vs. operating parameter at constant dimensionless thickness, t = 0.7. Constant dimensionless thickness implies constant travel speed, since t* = tv/2α. Weld penetration increases sharply with small increases in weld power when the weld nears full penetration.*

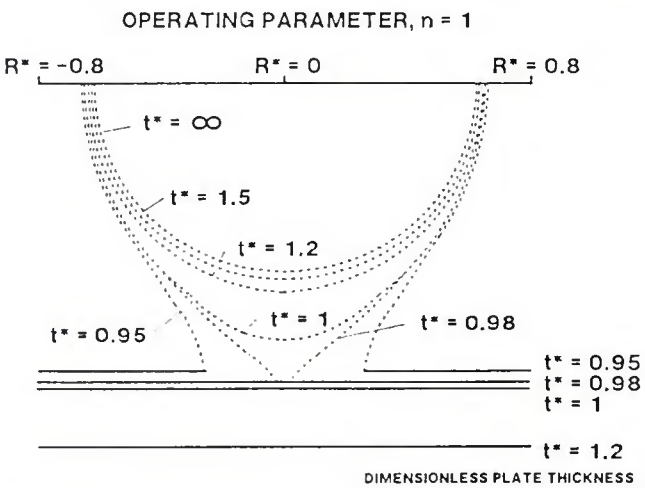

Fig. 2 — Calculated weld penetration of a 3-D heat flow weld (point source) vs. plate thickness at constant operating parameter, n=1. The dimensionless thickness t = tv/2α, and R* = Rv/2α. Weld penetration increases sharply for small decreases in plate thickness when the weld is near full penetration.*

flow around both arc and deep penetration weldments were performed. For arc sources, these calculations assumed that 3-D heat flow applies and therefore used the Rosenthal equation as a starting point. An image heat source a distance 2t below the source was used to simulate the back surface boundary condition, as described by Myers, *et al.* (Ref. 1). This approach gives a very good approximation to the solution for heat flow in a finite plate. An exact solution requires a series of image sources both above and below the plate, but for the plate thicknesses employed here the difference between the exact solution and the single image source approximation is negligible. A plot of calculated weld pool shape for increasing operating parameter n is shown in Fig. 1. At a constant operating parameter, the effect of changing plate thickness on calculated weld pool shape is shown in Fig. 2.

It is apparent from both Figs. 1 and 2 that, near full penetration, small changes in operating parameter or plate thickness are expected to produce large changes in joint penetration. The change in penetration for a small change in welding current, travel speed, and plate thickness was calculated for a semi-infinite plate and for a thin plate at 80% and 95% penetration. The results are given in Table 1. The increased sensitivity of weld penetration to changes in welding conditions is dramatic when the weld is near full joint penetration.

As indicated previously, the analytic solution for three-dimensional heat flow can be improved by treating the arc as a distributed rather than a point heat source. A limited number of numerical solutions (Ref. 11) to the heat flow equations were obtained, with the addition of an image distributed heat source to simulate the back surface boundary condition. These solutions are compared in a subsequent section with those obtained using the point source approximation and with experimental observations.

Increased penetration sensitivity at the approach to full penetration can also be seen in welding processes that are described by nearly two-dimensional heat flow. These are welds where little of the input power is transported in the part vertical direction. Examples of this are deep penetration EB and laser beam welds. Even though little of the heat is moving in the part thickness direction, some heat flow occurs in the vertical direction and somewhat increased penetration can result when approaching full penetration.

In order to numerically simulate increased penetration for deep penetration welding, the heat source was approximated as a line of point sources extending partially through the plate (1000 sources were used in order to give a reasonable numerical approximation of an actual line source). Each point source represents the appropriate fraction of total input power. At any location in the part, the temperature is a sum of the individual temperatures from each of the point sources. Part backside effects were simulated by a similar line of image heat sources starting a distance 2t below the plate top surface and extending toward the plate back surface to form a mirror image of the actual source. Again, the difference between this approximation and the exact solution using multiple sets of image sources is negligible for the plate thicknesses tested. The basic result of this calculation was that only a small penetration increase is expected near to full penetration. This is reasonable since only a small fraction of the input power is situated near enough to the plate back surface to feel the effects of finite thickness. Unfortunately, the predicted weld penetration increase using this model is too small to describe the experimental data.

Table 1—Calculated Sensitivity of Weld Penetration to Small Changes in Welding Current, Travel Speed and Plate Thickness at Different Fractional Penetration.

	Δd/d (Thick plate)	Δd/d (80% penetration)	Δd/d (95% penetration)
Current	0.6 Δl/l	2.4 Δl/l	4.2 Δl/l
Travel Speed	−0.4 Δv/v	−1.6 Δv/v	−2.8 Δv/v
Thickness	0.0 Δt/t	−4 Δt/t	−6 Δt/t

The discrepancy between calculations and experiment can be reconciled if we notice that in an actual deep penetration weld, the length of the line source is essentially equal to the weld penetration. Thus, the length of the line heat source will increase a bit if the weld penetration increases due to a finite thickness effect. When this happens the heat source approaches closer to the plate back side and the penetration will increase even more. This cooperative interaction between heat source position and weld penetration means that sensitivity of penetration to changes in heat source can be reasonably large. Note that it is possible to arrive at a stable weld penetration even when heat buildup at the part backside becomes important. This is possible because an increase in source length decreases the power density and the liquid metal will start to cool somewhat, especially near the top surface. A balance between enhanced penetration, caused by finite thickness, and decreasing power density can normally be achieved, except quite near to full penetration.

The source length change phenomenon in beam welding was modeled by assuming a particular input power and calculating the temperature a lateral distance, equal to the beam radius, away from the bottom-most point source in an infinitely thick plate. Then, for the same input power in a finite thickness plate, line source length was increased to achieve the same temperature at the same place. The calculated dimensionless temperature [$\theta = T(r) - T_O/(T_f - T_O)$] at the same place was $\theta = 1.3$. Results of this calculation are shown in Fig. 3.

This is a plot of expected penetration vs. input operating parameter at sharp focus (r = 0.16 mm). Notice that, unless

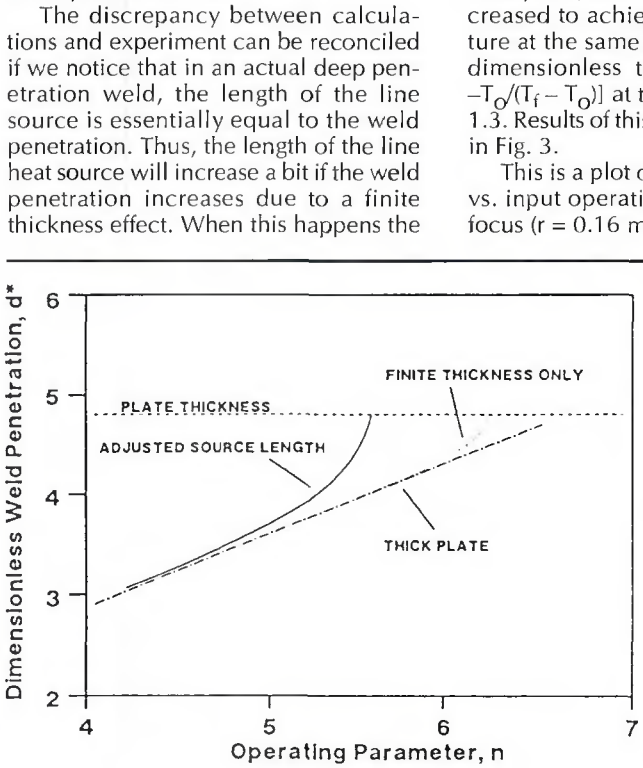

Fig. 3 — Calculated weld penetration of a 2-D heat flow weld (line source) vs. beam current (operating parameter) for a thin plate specimen. Notice that penetration is predicted to increase linearly with beam power until it becomes about 0.8 times the plate thickness. Calculated penetration enhancement is shown for the constant and variable source length models. The dimensionless penetration $d^* = dv/2\alpha$. The calculations are for a dimensionless beam radius ($rv/2\alpha$) of 0.4).

the bottom surface is near, the line source length only needs to increase a small amount to achieve equilibrium. Near to the bottom surface, the deep penetration weld is seen to rapidly move to full penetration. These calculated penetration values are in reasonable agreement with experiment and confirm that source length must be properly adjusted to model the finite thickness effect in deep penetration welding.

Experimental Procedures

Arc weld data obtained for this study were from autogenous GTA welds on Type 304L stainless steel. Welds were made in a constant current mode using a high precision GTAW power supply. No automatic voltage control (AVC) or current pulsing were used in these tests. The process parameters studied were: part thickness, arc current, part travel speed, arc length and arc voltage.

It is recognized that this is not an exhaustive list of parameters, but these are sufficient to provide basic quantitative sensitivity data for GTA welding.

Tapered Section Plate

In order to test the effects of material thickness in a simple way, a variable thickness weld specimen was used. The specimen was made by cutting a 100-mm (4-in.) wide and 150-mm (6-in.) long plate so that it was tapered uniformly from 8 mm (0.31 in.) thick on one end to 2 mm (0.08 in.) thick on the other. This tapered section specimen is useful because a continuous weld made along the length of the plate tests effects of thickness on weld penetration over a wide range of conditions. In addition, a single longitudinal metallographic section of the tapered specimen shows the thickness effect in convincing fashion. Of course, a tapered specimen cut at an excessive angle would not allow the bottom surface heat buildup to occur normally and the results would not be valid. The shallow angle of this tapered specimen and the relatively slow travel speed used in these tests makes results quoted here valid.

The parameters used to generate the tapered section weld data were: weld current, 190 A; travel speed, 3 mm/s (7 in./mm); arc length, 1.5 mm (0.06 in.); cover gas, pure argon; electrode, 3/32 in. (2.5 mm) ground to sharp 30-deg tip angle.

Note that these weld parameters correspond to an approximate value of operating parameter of n = 2. A longitudinal metallographic section as well as several transverse sections of the resulting weld were produced and the penetration was measured as a function of plate thickness.

GTA Welding Parameter Tests

The effects of welding parameter variations on weld penetration were tested using a thin flat-section specimen of Type 304L stainless steel, that was 2.35 mm thick (0.09 in.). A baseline set of parameters was established that would produce full joint penetration with limited drop-through. The baseline parameters were: weld current, 75 A; travel speed, 2.5 mm/s (6 in./s); arc length, 1.27 mm (0.05 in.), 8.1 V; cover gas, pure argon; electrode, 3/32 in., ground to sharp 30-deg tip angle.

This set of welding parameters corresponds to an operating parameter of about 0.65. At these conditions, full joint penetration welds were made with drop-through that was about 0.05 mm (0.002) deep and about 1.1 mm (0.04 in.) wide. Small parameter variations away from the baseline value were found to produce significant variations in weld penetration.

Welding variables were varied around the baseline conditions to produce a range of weld penetration values. Each parameter was tested in turn in a one-variable-at-a-time experiment. A transverse metallographic section was made of each weld and weld penetration and width were measured directly from the section. Note that measured values of penetration greater than the 2.35 mm plate thickness represent plate thickness plus measured weld drop-through.

Electron Beam Welding Parameter Tests

A limited series of EB welds were made in the same 2.35-mm-thick Type 304L stainless steel plate. A baseline set of parameters was established that would produce near full penetration welds and these baseline parameters were: beam voltage, 110 kV; beam current, 4 mA; travel speed, 17 mm/s (40 in./min); beam focus, sharp focus.

Using these weld parameters, weld penetration was about 1.8 mm and was found to be quite sensitive to small parameter variations that increased input power density away from the baseline value.

Weld parameters were varied around the baseline conditions in a one-variable-at-a-time experiment. A transverse

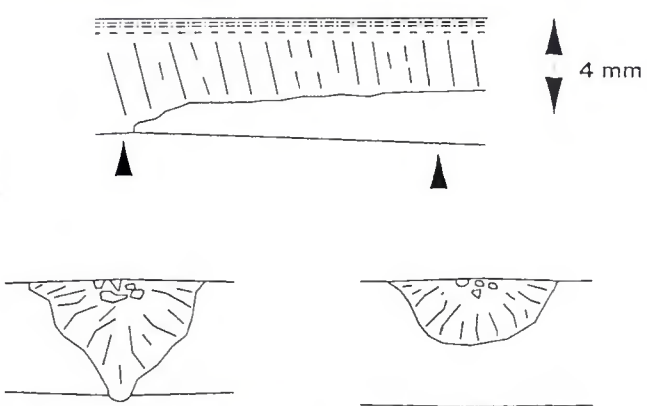

Fig. 4 — Metallographic sections of the tapered section specimen. Notice the nearly constant penetration on the thick side of the specimen and the rapid increase toward full penetration at the thin end. The arrows indicate locations of the transverse cross-sections.

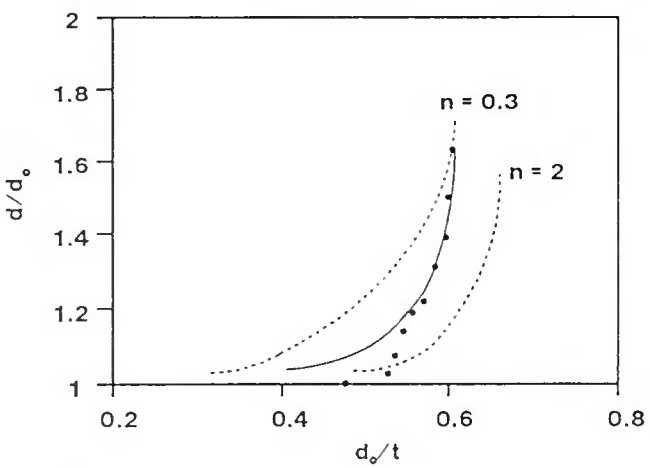

Fig. 5 — Weld penetration d as a function of material thickness t measured from the tapered section specimen. d_o is the penetration for a semi-infinite plate for the same welding conditions. The dashed curves are theoretical predictions of penetration enhancement for a point source. The solid line is the theoretical prediction for a distributed source with dimensionless size U = 0.35 and operating parameter n = 2.

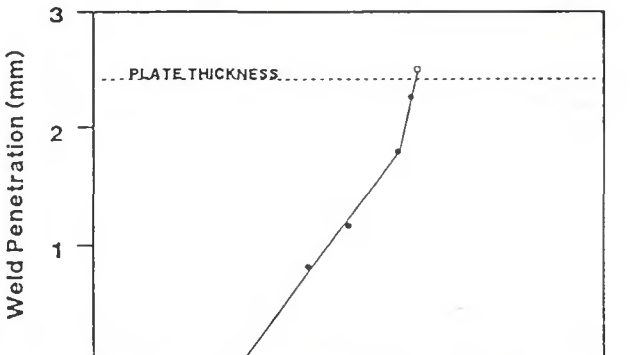

Fig. 6 — Weld penetration vs. welding current showing the very large sensitivity of penetration to current near to the material thickness.

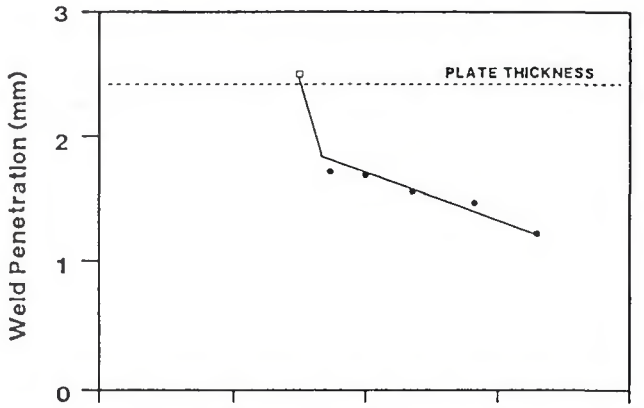

Fig. 7 — Weld penetration vs. travel speed showing the large penetration sensitivity for near to full penetration welding.

metallographic section was made of each weld and weld penetration and width were measured directly from the section. Note that measured values of penetration greater than the 2.35-mm plate thickness represent plate thickness plus measured weld root penetration. It was found that weld penetration was most sensitive to beam focus condition and to beam power. The sensitivity to the other weld parameters was significant but was somewhat less. Only beam power data are discussed in this paper.

Results and Discussion

Part Thickness

The tapered section plate was utilized to test effects of thickness changes on weld penetration. Tracings of weld micrographs are shown in Fig. 4. Note that penetration is nearly constant at the thick end of the section. As plate thickness decreases, weld penetration increases rapidly toward full penetration. The fingers of penetration at the weld midline, seen in the full penetration transverse section, is similar in shape to that predicted by the heat flow analysis — Fig. 2.

Measurements of weld penetration as a function of plate thickness were made from the longitudinal metallographic section and are shown in Fig. 5. The weld was made at a constant operating parameter, n = 2. Theoretical predictions of penetration enhancement vs. plate thickness are also shown in Fig. 5. The dashed lines are predications from a traveling point heat source (the Rosenthal solution), and the solid line is the predicted penetration enhancement for a traveling distributed heat source with operating parameter n = 2. For the distributed source, the dimensionless arc size $U = v\sigma/2\alpha$ was taken to be 0.35. The actual arc size σ used to determine U was taken from measurements reported in Ref. 12 for essentially the same welding conditions.

A comparison of calculated (point source) and observed slopes of penetration vs. thickness for thick plate and for thin plate at 95% penetration is given in Table 2. Agreement between experimental penetration enhancement and the theoretical prediction is good. As expected, agreement between calculated and experimental penetration enhancement is improved substantially by treating the heat source as distributed rather than as a point. The distributed nature of the actual heat source makes lateral heat transfer more difficult near full penetration, so penetration enhancement begins at lower relative penetration than predicted by the point source approximation.

Weld Current

The thin flat-plate specimen was used to evaluate effects of current variations on weld penetration. Weld current was varied in these tests between 35 A, where the onset of melting occurred, and 120 A, where very strong drop-through was observed. Full penetration was observed to occur at about 73 A. Weld penetration vs. current is shown in Fig. 6. Near full penetration, the slope of the penetration vs. current curve increases sharply. The slopes measured near 95% penetration are compared to those predicted by the heat flow analysis in Table 2. Experimental and calculated penetration sensitivities with current are in reasonable agreement.

Travel Speed

Sensitivity of weld penetration to travel speed was tested using the thin flat-plate specimen. Travel speed was varied between 1.9 mm/s (5 in./min), where significant drop-through was observed, to 4.3 mm/s (10 in./min) where penetration was about one-half of the plate thickness. Weld penetration vs. travel speed is shown in Fig. 7. As with current, the slope of the penetration vs. travel speed plot changes sharply as full penetration Is approached. Measured slopes are compared to those predicted by the heat flow analysis in Table 2.

Arc Length

The weld penetration dependence on arc length was also tested with the thin flat-plate specimen. Arc length can affect weld penetration because an increase in arc length will make the arc broader and will generally produce a

Table 2—Comparison of Experimental and Calculated Change of Weld Penetration per Unit Change in the Process Parameters. Point Source Approximation.

	Semi-infinite Plate		Thin Plate at 95% Penetration	
	Measured	Calculated	Measured	Calculated
Thickness	0.0	0.0	−5	−6
Current	0.05 mm/A	0.02 mm/A	0.20 mm/A	0.14 mm/A
Travel Speed	$-0.5\ s^{-1}$	$-0.4\ s^{-1}$	$-2.4\ s^{-1}$	$-2.8\ s^{-1}$
Arc Length	−0.5		−0.9	

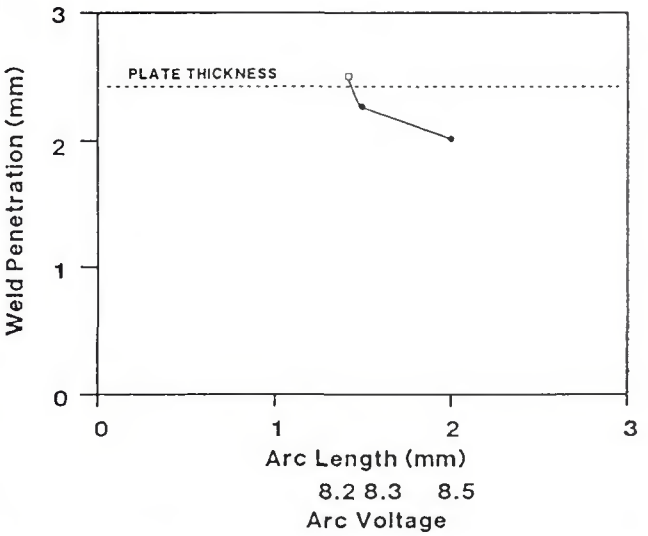

Fig. 8 — Weld penetration vs. arc length. Also shown are the arc voltage values obtained at the corresponding arc lengths.

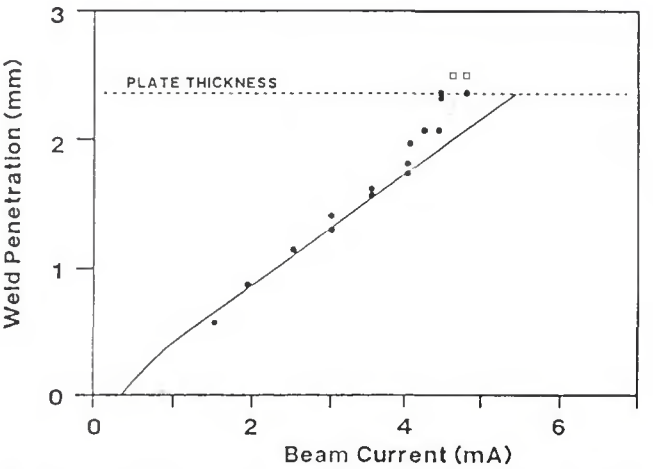

Fig. 9 — Weld penetration vs. beam current for electron beam welds made at sharp focus and with V = 110 kV and v = 17 mm/s. The solid line shows the penetration behavior for thick plate. The dashed line is the calculated penetration from the finite thickness, adjusted source length, 2-D heat flow model.

wider and shallower weld. This effect was tested by varying arc length between 0.5 mm, where significant drop-through occurred, and 1.9 mm, where joint penetration was significantly less than material thickness. Weld penetration vs. arc length is shown in Fig. 8. It seems that the increase in sensitivity of weld penetration to arc length is small near full penetration, as would be expected of a variable that has only an indirect effect on weld penetration. The numerical value of sensitivity of weld depth to arc length near full penetration is given in Table 2. Note that this sensitivity value lacks precision since only three data points were obtained for arc length. No theoretical value of this sensitivity is presented since the calculations do not include any effects of source size.

There may be many other process variables in arc welding that are normally of only limited importance but become relevant when enhanced by finite plate heat flow. Examples of this are material chemistry fluctuations, and heat-sinking variations. The critical concept is that any process change, even if normally very subtle, will be enhanced greatly in the vicinity of full penetration. Unpredictable penetration can easily result when operating in this unstable regime.

Electron Beam Welds

To illustrate that finite thickness effects can occur in other processes, a few electron beam welds were made on the thin flat-plate specimen. The only EBW process parameter discussed here is beam power. Beam power was varied by maintaining constant beam voltage and focus condition and simply changing beam current between 1 and 5 mA. From 1 to 4 mA, weld penetration was found to increase linearly with increasing current. For beam current greater than 4 mA, penetration increased more rapidly toward full penetration. The data that show the rapid increase toward full penetration are shown in Fig. 9. Electron beam weld penetration has a correspondingly high sensitivity to other process parameters such as beam focus and travel speed; these data will be presented elsewhere. Also shown in Fig. 9 is the finite thickness penetration enhancement curve calculated with the adjusted source length model outlined in the Heat Flow section of this paper. The fit of calculations to the data is quite good and illustrates that the finite thickness perturbation of heat flow is important for processes described by 2-D heat flow. The data also confirm that the change in line source length must be included in a heat flow calculation to properly describe the finite thickness effect.

Conclusions

Substantial joint penetration variations are often observed near full penetration for both arc and electron beam welding processes. The fundamental origin of this variability is the transition from three-dimensional to two-dimensional heat flow away from the weld as full penetration is approached. In this transition regime, penetration depends very sensitively on the exact welding conditions. The sensitivity of penetration to current, voltage, travel speed, and thickness has been measured for GTA welds near full penetration in 304L stainless steel. These sensitivities are substantially greater than those measured far from full joint penetration. Similar results were obtained for electron beam welds in the deep-penetration mode.

Experimental results are in reasonable agreement with predictions from exact solutions to the conduction equations for finite thickness plate using a point or line heat source. Excellent agreement is achieved when the arc is treated as a distributed rather than a point heat source. For the partial joint penetration line source solution, the length of the source must be increased as penetration increases. When this is done, excellent agreement is achieved between calculated and measured weld penetration. Agreement between experimental and calculated penetration is achieved because a tightly focused electron beam is closely approximated by a line heat source. The agreement between experimental results and calculations suggests that increased sensitivity to welding conditions will be observed near full joint penetration for all welding heat sources.

Acknowledgment

This work was supported by the Department of Energy, Albuquerque Operations Office. Their support is gratefully acknowledged.

References

1. Myers, P. S., Uyehara, O. A., and Borman, G. L. 1967. Fundamentals of heat flow in welding. Welding Research Council Bulletin 123, New York.

2. Rosenthal, D. 1941. Mathematical theory of heat distribution during cutting and welding. *Welding Journal* 31(5):220-s to 234-s.

3. Christensen, N. V., Davies, V. de L., and Gjermudsen, K. 1965. Distribution of temperatures in arc welding. *British Welding*

Journal 12(12): 54–75.

4. Savage, W. F., Nippes, E. F., and Zanner, F. J. 1978. Determination of GTA weld-puddle configurations by impulse decanting. *Welding Journal* 57(7):201-s to 210-s.

5. Roberts, D. K., and Wells, A. A. 1954. Fusion welding of aluminum alloys: Part V - A mathematical examination of the effect of bounding planes on the temperature distribution due to welding. *British Welding Journal* 1:553–560.

6. Malmuth, N. D., Hall, W. F., Davis, B. I., and Rosen, C. D. 1974. Transient thermal phenomena and weld geometry in GTAW. *Welding Journal* 53(9):388-s to 400-s.

7. Friedman, E., and Glickstein, S. S. 1976. An investigation of the thermal response of stationary gas tungsten arc welds. *Welding Journal* 55(12):408-s to 420-s.

8. Alberry, P. J., Anderson, I. M., and Brunnstrom, R. R. L. 1988. Weld penetration variability in manual and mechanized thin section 9Cr-1Mo tube attachment welds. *Sheet Metal Industries* 65(1):5–16,18,20.

9. Jhaveri, P., Moffatt, W. G., and Adams, C. M. 1962. The effect of plate thickness and radiation on heat flow in welding and cutting. *Welding Journal* 41(2):12-s to 16-s.

10. Barry, J. M., Paley, Z., and Adams, C. M. 1963. Heat conduction from moving arcs in welding. *Welding Journal* 42(3): 97-5 to 104-s.

11. Heiple, C. R., and Roper, J. R. 1990. The geometry of gas tungsten arc, gas metal arc, and submerged arc weld beads. *Welding: Theory and Practice*. Eds. D. L. Olson, R. Dixon, and A. L. Liby, pp. 1–34. Amsterdam: Elsevier.

12. Smartt, H. 1990. Arc-welding processes. *Welding: Theory and Practice*. Eds. D. L. Olson, R. Dixo, and A. L. Liby, pp. 175–208. Amsterdam: Elsevier.

WRC Bulletin 336
September 1988

Interpretive Report on Dynamic Analysis of Pressure Components—Fourth Edition

This fourth edition represents a major revision of WRC Bulletin 303 issued in 1985. It retains the three sections on pressure transients, fluid structure interaction and seismic analysis. Significant revisions were made to make them current. A new section has been included on Dynamic Stress Criteria which emphasizes the importance of this technology. A new section has also been included on Dynamic Restraints that primarily addresses snubbers, but also discusses alternatives to snubbers, such as limit stop devices and flexible steel plate energy absorbers.

Publication of this report was sponsored by the Subcommittee on Dynamic Analysis of Pressure Components of the Pressure Vessel Research Committee of the Welding Research Council. The price of WRC Bulletin 336 is $20.00 per copy, plus $5.00 for postage and handling. Orders should be sent with payment to the Welding Research Council, Suite 1301, 345 E. 47th St., New York, NY 10017.

WRC Bulletin 357
September 1990

Calculation of Electrical and Thermal Conductivities of Metallurgical Plasmas

By G. J. Dunn and T. W. Eagar

There has been increasing interest in modeling arc welding processes and other metallurgical processes involving plasmas. In many cases, the published properties of pure argon or helium gases are used in calculations of transport phenomena in the arc. Since a welding arc contains significant quantities of metal vapor, and this vapor has a considerably lower ionization potential than the inert gases, the assumption of pure inert gas properties may lead to considerable error. A simple method for calculating the electrical and thermal conductivities of multicomponent plasmas is presented in this Bulletin.

Publication of this report was sponsored by the Welding Research Council. The price of WRC Bulletin 357 is $20.00 per copy, plus $5.00 for U.S. or $10.00 for overseas postage and handling. Orders should be sent with payment to the Welding Research Council, 345 E. 47th St., New York, NY 10017.